

# Mixed signal controller for an experimental magnetotherapy device

Paweł Pawłowski, and Marek Portalski

**Abstract**—The article presents the design of a controller for an experimental magnetotherapy device. The controller realizes precise, digital generation of a 3-phase sinusoidal signal with a frequency of 1 Hz to 5 kHz and slowly variable frequency modulation of 1 Hz to 5 Hz, which is a novelty in the field of magnetotherapy. The structure and operation of the analog filter path and the regulation of the amplitude and the DC component are discussed. A fast STM32F334 microcontroller was used to generate the signal, and an ATmega2560 microcontroller was used to operate the user interface with a color touch display. Laboratory and therapeutic tests confirmed proper operation of the controller.

**Keywords**—controller; digital signal generation; magnetotherapy; reconstruction filter

## I. INTRODUCTION

MAGNETOTHERAPY is a procedure in the field of physical medicine that allows for treatment with a magnetic field [1]-[4]. It uses the positive effect of a variable magnetic field on the human body. Unlike magnetostimulation, it involves the use of a magnetic field with higher intensity in continuous or pulsed mode [2]. In Poland, typically low-frequency magnetic fields are used in therapy, mainly in the range of 0 to 50 Hz. Only in new types of devices do the frequencies go beyond this range. For example, BTL series 4000 and 5000 devices have a working range of up to 166 Hz [5]. However, it should be noted that research conducted long ago showed the existence of many resonance frequencies in the human body. For example, the works of Nogier, Kroy and Bahr provide entire tables of such frequencies reaching 10 kHz [6],[7]. Signals with frequencies in the kHz range are often used, for example, in electroacupuncture and laser therapy.

Devices with modulated magnetic field frequency are rare. An exception is the Czech RENAISSANCE Duo Forte device, where modulation was realized with a slowly changing sawtooth waveform in the ranges of 2 Hz - 25 Hz, 5 Hz - 45 Hz and 35 Hz - 60 Hz [8],[9].

The authors of this article have not yet encountered a magnetotherapy device using a rotating field generated by a system of coils powered by three-phase current. Therefore, it was decided to design and build a magnetotherapy device controller generating a three-phase signal with modulated frequency and the possibility of adding a constant component to the signal. Such a controller, after supplementing it with an

appropriate high-power current amplifier and special multi-coil applicators, can be used in the future for experimental work in the field of new techniques and applications of magnetotherapy.

## II. A CONTROLLER – TECHNICAL ASSUMPTIONS

The developed magnetotherapy controller should enable conducting tests and therapies in a wide range of generated signal frequencies, while, at the same time, ensuring convenient and clear operation. The following technical assumptions were stated:

- Generation of a 3-phase sinusoidal signal with the possibility of switching the phase shift of magnetic field into one of three modes: static, left-handed and right-handed.
- Field mode can be switched during operation and indicated by light-emitting diodes (LEDs).
- Signal frequency range from 1 Hz to 5 kHz with minimum resolution of 0.1 Hz in the signal range up to 100 Hz, and minimum 1Hz above 100 Hz.
- Frequency modulation (FM) option, made simultaneously in all channels:
  - FM frequency from 0.1 Hz to 5 Hz,
  - FM deviation from 0 to max 30%,
  - FM modulating signal: symmetrical triangle.
- Signal amplitude at the outputs (the same for all channels) adjustable from 0 to max 2 V.
- Hardware signal switching into two sub-ranges: one from 0 to 0.5 A and second from 0 to 1.5 A.
- Two knobs for adjustment: one for signal (carrier) frequency, modulation frequency and deviation (e.g. an optical rotary encoder), second for the output current (analog potentiometer with a digital readout of the position).
- Large digital display (color, touch-controlled), with all the parameters displayed.
- Manual (hardware) Start / Stop switch.
- The controller have to be autonomous, i.e. without the need a computer to work.

## III. ANALOG AND DIGITAL SIGNAL GENERATION

The generation of a single sinusoidal signal with the above parameters could be realized using analog circuits. However, assuming a tunable 3-phase signal with precisely defined phase shifts, this would require the use of three synchronized generators or a single generator with a phase shifter. The

This work was supported by a research subsidy 0211/SBAD/0224.

Paweł Pawłowski is with Division of Signal Processing and Electronic Systems, Institute of Automatic Control and Robotics, Poznan University of Technology, Poland (e-mail: pawel.pawlowski@put.poznan.pl, <https://orcid.org/0000-0001-5373-5148>).

Marek Portalski, is an independent researcher (e-mail: [marek.portalski@outlook.com](mailto:marek.portalski@outlook.com)).



implementation of this type of generator would most likely be insufficiently stable in time, and also and complicated in terms of circuit complexity.

Digital signal generation would be much more accurate, more time-stable and easier to control. However, in the discussed controller (see Section II), it requires the use of accurate generation procedures (cf. frequency control requirements), a sufficiently fast processor and three digital-to-analog converters (DACs). The authors, having extensive experience in designing both analog and digital systems [10]-[12], proposed a hybrid solution. In consequence, the signal generation with an option of the frequency modulation was carried out digitally, but the circuit for adding a constant (DC) component and amplitude control was implemented in the analog path. This allowed the use of DACs with a lower resolution, while maintaining a low level of distortion in the entire range of useful amplitudes.

The block diagram of the entire digital signal controller for an experimental magnetotherapy device is shown in Fig. 1.

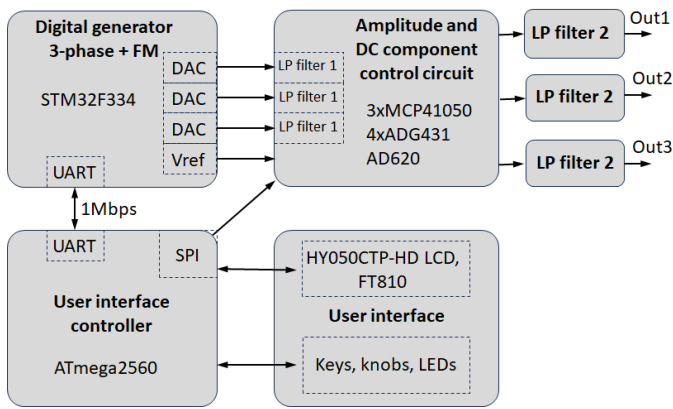


Fig. 1. Block diagram of the digital signal controller for an experimental magnetotherapy device

#### IV. A SIGNAL CONTROLLER

As mentioned above, the signal generation controller is composed of two parts: digital and analog.

##### A. Digital part

When we decided on digital generation of a sinusoidal signal, we could implement it in several ways. The most important methods of digital signal generation include: direct digital synthesis (DDS), the use of an unstable filter with an infinite impulse response (IIR filter), the use of the inverse Fourier transform (e.g. in fast version, i.e. IFFT) or the approximation of the sine function with phase accumulation. Only the last method allows for a relatively simple implementation of an additional slowly varying frequency modulation. Therefore we used this method. The  $n$ -th sample of a single signal  $x_n$  is calculated as follows [13]:

$$x_n = A \cdot \sin(\varphi_n) \quad (1)$$

$$\varphi_n = \varphi_{n-1} + W_g \quad (2)$$

$$W_g = 2\pi \cdot T_s \cdot f_g \quad (3)$$

where:

$A$  – signal amplitude,

$f_g$  – signal frequency

$T_s$  – sampling period.

The generation of a signal composed of three components with the same frequency and amplitude but different phases can be realized using one phase accumulator  $\varphi_n$  and a three-fold approximation of the sine function with an appropriate phase correction:

$$x_{n1} = A \cdot \sin(\varphi_n + \Delta\varphi_1) \quad (4)$$

$$x_{n2} = A \cdot \sin(\varphi_n + \Delta\varphi_2) \quad (5)$$

$$x_{n3} = A \cdot \sin(\varphi_n + \Delta\varphi_3) \quad (6)$$

For a stationary magnetic field:

$$\Delta\varphi_1 = \Delta\varphi_2 = \Delta\varphi_3 = 0 \quad (7)$$

For a clockwise rotating magnetic field:

$$\Delta\varphi_1 = 4/3\pi; \Delta\varphi_2 = 2/3\pi; \Delta\varphi_3 = 0 \quad (8)$$

For a counter-clockwise rotating magnetic field:

$$\Delta\varphi_1 = 0; \Delta\varphi_2 = 2/3\pi; \Delta\varphi_3 = 4/3\pi \quad (9)$$

Additional frequency modulation (FM) with a triangular modulating signal, simultaneously in all channels, can be achieved using phase accumulator correction according to the following relations:

$$\varphi_n = \varphi_{n-1} + W_g \cdot (M_n + 1) \quad (10)$$

$$M_n = M_{n-1} + W_m \quad (11)$$

$$W_g = 2\pi \cdot T_s \cdot f_g \quad (12)$$

$$W_m = \pm \frac{4 \cdot g \cdot f_m}{f_s} \quad (13)$$

where additionally:

$g$  – frequency deviation

$f_m$  – modulating signal frequency

The sign of  $W_m$  changes every half period of the modulating signal.

Since, according to the assumptions stated in Section II, the controller is to operate autonomously (without the need to connect a computer), the above calculations had to be performed using a signal processor or a suitably fast microcontroller. In order to reduce the costs of the prototype, as well as the costs of potential production of the device, a microcontroller with built-in DACs was taken into account during a device selection.

When analyzing the offers of various manufacturers, finding a microcontroller with three built-in DACs turned out to be a difficult task. Ultimately, the STM32F334R8 chip from the STM32 family from STMicroelectronics was selected. The STM32 family is extensive and offers 32-bit microcontrollers with different architectures and a wide range of built-in peripherals. The STM32F334R8 microcontroller is based on a computing core from the ARM Cortex-M4 series, can operate at a clock speed of up to 72 MHz and has built-in 3 DACs and 2 analog-to-digital converters (ADCs), all with a resolution of 12 bits. Using the full dynamics of the converters, this gives a theoretical signal-to-noise ratio of about 72 dB. This is sufficient in the discussed application. However, to avoid to avoid distortions caused by quantization errors it requires converting a full-scale of the signal amplitude and regulation of both the amplitude and the additional DC component in the analog path.

The STM32F334R8 microcontroller software was written in the Mbed environment in C/C++ programming language [14]. Mbed is a development platform and operating system for devices based on 32-bit ARM Cortex-M microcontrollers and it allowed software to be written and compiled online, without

having to install a development environment on the programmer's computer. The project was a collaboratively developed by Arm and its technology partners.

In order to obtain the assumed precision in signal quality and setting the parameters of the generated signal, 32-bit floating-point arithmetic was used. The 32-bit precision is sufficient to implement the described algorithm with assumed accuracy and is hardware supported by the selected microcontroller. This is very important because any software implementation of calculations on longer words (e.g. 64-bit) significantly reduces the maximum speed of signal generation.

After optimizing the generator software code, a stable generation speed of 25 kS/s (samples per second) was achieved with the possibility of changing parameters sent via the UART interface during generation. The code used 30.7 kB of 64 kB built-in FLASH memory and 1.9 kB of 8 kB of RAM of the microcontroller.

### B. Analog part

The following circuits were built in the analog part of the controller:

- amplitude control circuit with digitally programmable analog attenuators.
- DC component addition and control circuit,
- low-pass reconstruction filter (for each of the three channels).

The reconstruction filter was divided into two parts. The first part was placed right after the DAC, while the second one was placed after the amplitude control and DC component addition circuit. The first part is designed to initially eliminate interference from the digital part of the system. The second part finally shapes the filter characteristics and additionally removes interference that may appear in the digitally controlled amplitude control system, including transients when changing gain settings.

#### 1) Amplitude and DC component control circuit

The amplitude control and DC component addition circuit was implemented using operational amplifiers TLV2462 from Texas Instruments, digitally controlled potentiometers MCP41050 from Microchip Technologies, quadruple analog switches ADG431, and an instrument amplifier AD620 - both manufactured by Analog Devices.

A part of the circuit diagram of the amplitude control and constant component addition circuit for channel number 3 is shown in Fig. 2. The TLV2462 operational amplifiers (two of them for each channel) realize a voltage follower (to separate output impedance of the DAC from the filter the first part of the reconstruction filter. The additional TLV2462 precisely amplifies the reference voltage taken from the DAC to set the DC component. Digitally controlled potentiometers MCP41050, with 256 values of adjustable resistance and control via SPI interface, scale the software-set amplitude of sinusoidal signals and the DC component separately. The quadruple analog switches ADG431 configure the DC component and AC signal adder circuit, which is implemented on the AD620 instrument amplifier (with precisely set gain).

Controlling the amplitude regulation circuit and adding a DC component turned out to be a non-trivial task. The signal generated by the DAC, built into the microcontroller, is only positive, in the range of 0 to 3.3 V. To properly convert a sinusoidal signal (which is symmetrical about zero), a constant

component equal to the signal amplitude must be added to it (see Fig. 3).

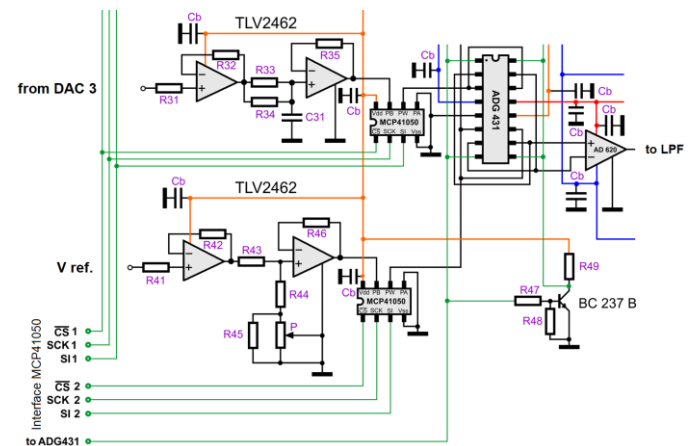


Fig. 2. A part of the diagram of the amplitude and DC component control circuit for channel number 3

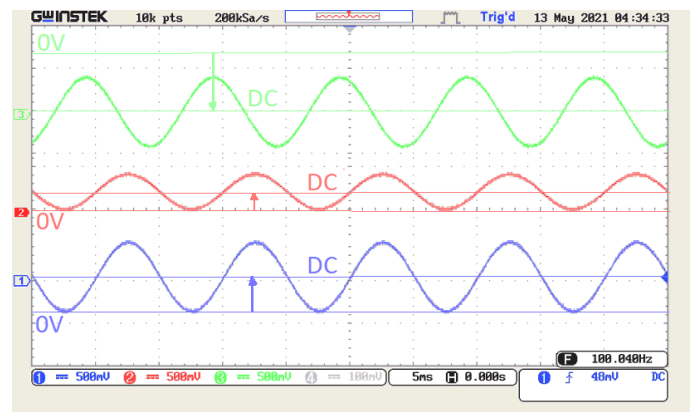


Fig. 3. Three example signals: a) large negative DC component, output signal only negative, b), c) positive DC component equal to the signal amplitude

This task is performed by a digital generator. In order to avoid distortion at the limit values, the following values of the generated signal, generated by the DAC (for one channel), were assumed:

$$S_1 = 1,4025 \sin \omega t + 1,5675 \quad (14)$$

The output signal from the generator, which is amplified by the power amplifier, should be of the form:

$$S_2 = C_1(k_1 \sin \omega t + k_2) \quad (15)$$

where:

$k_1$  - regulated amplitude,

$k_2$  regulated DC component.

By assumption, the added DC component can be both positive and negative. Therefore, the following relations apply:

$$0 \leq (k_1 + |k_2|) \leq 1 \quad (16)$$

$$-1 \leq k_2 \leq 1 \quad (17)$$

Let us define additional parameters  $l_1$  and  $l_2$  that satisfy the following relations:

$$k_1 = l_1(1 - |l_2|) \quad (18)$$

$$k_2 = l_1 l_2 \quad (19)$$

By substituting the relations (18) and (19) into (15) we obtain the output signal  $S_2$  defined by the parameters  $l_1$ ,  $l_2$ , and  $C_1$ :

$$S_2 = C_1(l_1(1 - |l_2|)\sin\omega t + l_1l_2) \quad (20)$$

Signal  $S_2$  must be equal to the modified signal  $S_1$ , from which the DC component is subtracted or added to. For each variant of the operation (subtraction or addition) different formulas apply.

The solution to the problem should provide dependencies on 8-bit settings of digital potentiometers regulating the signal amplitude and the value of the added (or subtracted) DC component and variants of adding (or subtracting) signals set using analog switches.

After transformations, we obtain three variants of settings of two digital potentiometers  $N_1$  and  $N_2$ . The first variant is concerned with adding signals, the second with subtracting signals, and the third with subtracting of inverted signals. It was noticed that the variant with adding signals does not cover the entire range of regulation, therefore two variants were selected for implementation. First variant (with signal subtraction):

$$N_1 = 255 l_1(1 - |l_2|) \quad (21)$$

$$N_2 = 255(l_1 - l_1|l_2| - 0,89477 l_1l_2) \quad (22)$$

and second variant (with inverted subtraction of signals (instead of addition):

$$N_1 = 255 l_1(1 - l_2) \quad (23)$$

$$N_2 = 255 l_1(1 - 1,0523 l_2) \quad (24)$$

The above relations allow for full adjustment of the amplitude and the DC component, from the adopted ranges, regardless of their values. The microcontroller only needs to select the appropriate variant of operation, depending on the given input values.

## 2) Reconstruction filter

As it was mentioned above, the reconstruction filter was divided into two parts: the first part was placed right after the DAC, while the second one was placed after the amplitude control and DC component addition circuit. Together they realize the reconstruction filter.

With the assumed maximum signal frequency of 5 kHz and a deviation of 30% in FM, the maximum instantaneous frequency of the generated AC signal is 6.5 kHz. This gives a theoretical minimum sample generation rate of 13 kS/s. However, the theoretical solution does not leave any margin for the transition band of the reconstruction filter. The sample generation rate of 25 kS/s achieved by the STM32F334R8 microprocessor provides sufficient margin for the implementation of this filter.

The requirements for the reconstruction filter are met by a 5th order low-pass filter with Butterworth approximation and a cutoff frequency about 7 kHz. In practice, the filter is implemented in the Sallen-Key topology, in which one operational amplifier implements a filter of a maximum of 2nd order. Additionally, in order not to load the DAC output with the filter input impedance, and not to change the filter frequency response by the DAC output impedance, a voltage follower was added. Consequently, the filter (for one channel) consists of 4 operational amplifiers. The diagram of the reconstruction filter for one channel is shown in Fig. 4, and the calculated values of the filter elements are presented in Tab. I. The selection of operational amplifiers is described in Section VI.

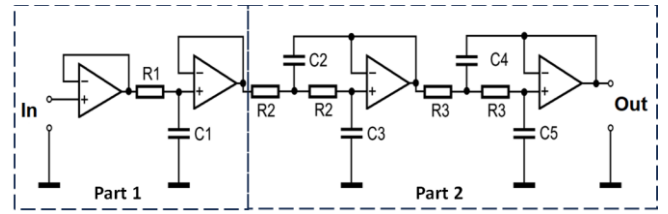


Fig. 4. The diagram of the 5th order reconstruction filter for one channel, divided into two parts 1 and 2

TABLE I  
EXACT VALUES OF FILTER ELEMENTS

R1	R2	R3	C1	C2	C3	C4	C5
[kΩ]	[kΩ]	[kΩ]	[nF]	[nF]	[nF]	[nF]	[nF]
12.626	8.462	15.851	1.800	3.320	2.173	4.640	443.1

## V. USER INTERFACE

The user interface, i.e. display, buttons and knobs, as well as signal generator settings adjustment in both the analog and digital parts of the signal controller (described in Section IV) are implemented by the additional microcontroller. The 8-bit ATmega2560 from Atmel (now Microchip Technology) was selected for this task. The separation of user interface and signal generation tasks into two microcontrollers allows for stable and efficient operation of the digital generator, which, apart from generation, is not burdened with any other tasks.

Communication between the microcontrollers is implemented via a serial UART interface (1 Mbps).

Unique codes of messages sent to the generator were proposed (ASCII coded characters, binary values):

- S, start of generation static magnetic field,
- P, start of generation of clockwise rotating magnetic field,
- L, start of generation of counter-clockwise rotating magnetic field,
- X, stop of generation,
- f, Frequency\_H, Frequency\_L - signal frequency (higher, lower byte) [0.1Hz],
- M, FMVal - modulating signal frequency (FM)
- D, DevVal\_H, DevVal\_L - frequency deviation (higher, lower byte) [0.1%],
- o, disable FM,
- O, enable FM,
- e, echo (ping), used for connection tests.

In the above encoding, the first symbol is unique, so different message lengths can be used.

For communication with the user, a 5-inch color touchscreen display HY050CTP-HD from HAOYU Electronics, with a resolution of 800x480, was used. The display has a built-in EVE (Embedded Video Engine) FT810 image controller from FTDI Chip. This controller allows for quick drawing of various graphic objects such as lines, circles, rounded rectangles, buttons. It also has built-in fonts of different sizes. The display was connected to ATmega2560 via SPI (serial peripheral interface).

The ATmega2560 microcontroller also supports an optical rotary encoder that performs the function of a digital value user input and, using the built-in ADC, reads and then displays the setting of the current control analog potentiometer. This setting affects the regulation of the signal amplitude, which is changed digitally in the analog path (described in details in Section IV).

The ATmega2560 microcontroller software was written in C/C++ programming language. The code used 20.6 kB of 256 kB built-in FLASH memory and 1.1 kB of 8 kB of RAM of the microcontroller.

Using the touch screen, the user can select the value they want to change, e.g. signal frequency or FM parameters, and then set the selected values using the knob.

The circuit has a voltage output and allows you to generate a voltage in the range of  $\pm 1.5V$ . Since the circuit directly drives a current amplifier that control coils generating a magnetic field with a gain of  $1A/1V$ , the user interface has an output signal scaled in Amps. The current settings are adjusted using a potentiometer, and the value is displayed on the screen. It is possible to select one of two ranges: 0 - 0.5 A or 0 - 1.5 A.

The phase sequence (cf. (7), (8), and (9)) of the output signals, which determine the magnetic field, is selected by means of three illuminated pushbuttons.

The next two buttons allow you to start and stop generation. The total generation time (therapeutic treatment) is displayed in the upper left corner of the screen. The design of the screen with touch buttons for Polish language users is presented in Fig. 5, while the entire front panel of the controller is shown in Fig. 6. Thanks to the built-in image processor functions of the FT810 controller, the look of the programmed screen is very close to its design.

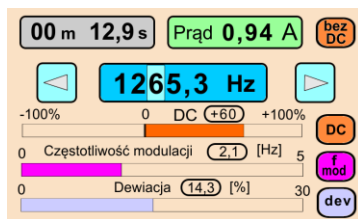


Fig. 5. Design of the screen with touch buttons



Fig. 6. User interface (front panel of the controller)

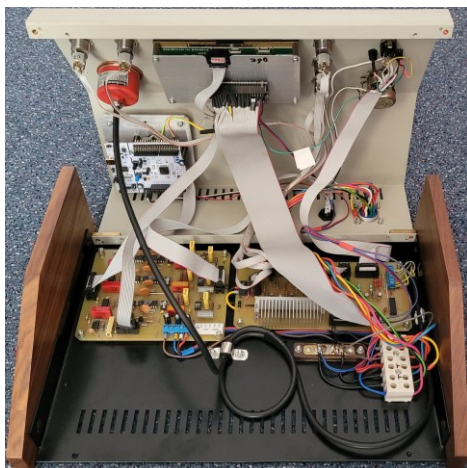


Fig. 7. Internal view of the realized controller

## VI. FUNCTIONAL TESTS AND MEASUREMENTS OF THE CONTROLLER

The presented controller was realized, tuned, and tested in terms of functionality and generated signals. The internal view of the controller is shown in Fig. 6.

### A. Reconstruction filter

After designing the reconstruction filter, its measurements were made. The filter was tuned to obtain the flattest passband and the most accurate representation of the theoretical frequency response. Finally, three filter versions were tested. Plots of the passband and the entire operating band measured during experiments are shown in Figures 7, 8, and 9. Detailed data on the passive elements are presented in Table II. Column 2 of Table II shows which components were used in a given filter version. For most components, a sufficient tolerance was 1-2%. The components R2a and C4a were selected experimentally, and their value may vary and depend on other factors, such as the PCB topology, the operational amplifiers used.

TABLE II  
REAL VALUES OF FILTER ELEMENTS

Element	Filter version	Nominal value	Tolerance	Measured value
R1	1,2,3	13.3 k $\Omega$	1 %	13.265 $\pm$ 0.005 k $\Omega$
R1a <sup>2</sup>	1,2,3	270 k $\Omega$	5 %	268.7 $\pm$ 0.3 k $\Omega$
R2	1,2,3	8.25 k $\Omega$	2 %	8.217 $\pm$ 0.001 k $\Omega$
R2a <sup>1,3</sup>	2,3	133 $\Omega$	2 %	-
R3	1,2,3	15.6 k $\Omega$	0.5 %	15.635 $\pm$ 0.005 k $\Omega$
C1	1,2,3	1800 pF	2 %	1800 pF
C2	1,2,3	3320 pF	2 %	3373 $\pm$ 1 pF
C3	1,2,3	2200 pF	1 %	2202 $\pm$ 3 pF
C4	1,2,3	4640 pF	1 %	4702 $\pm$ 3 pF
C4a <sup>1,4</sup>	3	180 pF	5 %	-
C5	1,2,3	453 pF	1.25 %	460 $\pm$ 1 pF

<sup>1</sup>Elements used in selected versions of the filter

<sup>2</sup>R1a is connected in parallel with R1

<sup>3</sup>R2a is connected in series with R2

<sup>4</sup>C4a is connected in parallel with C4

At the beginning, the filter was tested with the popular TL072 operational amplifiers. These are low-noise ( $V_n = 18nV/\sqrt{Hz}$ ), input field-effect transistors (FET) operational amplifiers, which offer gain-bandwidth product equal to 3 MHz [15].

Operational amplifiers with an input stage containing FETs are still one of the best solutions for low-noise amplifiers with gain-bandwidth sufficient to operate in the frequency range of several, a dozen or so kHz. Although better solutions are being developed, e.g. carbon nanotube field effect transistor (CNTFET), they are not yet used by manufacturers in discrete components [16].

Then, version 3 was rejected as the least accurate (c.f. Fig. 7), and versions 2 and 3 were additionally tested with the TLV2462 operational amplifiers (working in 1st section of the filter) and OP275 (working in 2nd and 3rd section of the filter).

The TLV2462 operational amplifier is a rail-to-rail type and is powered by a single +5V voltage [17]. This ensures that in transient states or interference it will not produce a voltage higher than 5V at the output, and therefore will not damage subsequent components in the signal path.

The OP275 operates with a bipolar signal and is powered by a voltage of  $\pm 15V$ . It is the first designed amplifier from

Analog Devices to feature the Butler amplifier front end. Its front end design combines both bipolar and JFET transistors to attain amplifiers with the accuracy and low noise performance of bipolar transistors, and the speed and signal quality of JFETs. The gain-bandwidth product is equal to 9 MHz and noise  $V_n = 6nV/\sqrt{Hz}$  [18].

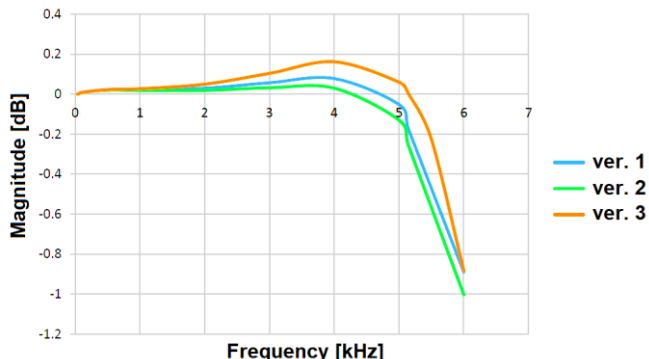


Fig. 7. Pass-band filter frequency response for TL072 operational amplifiers in 3 versions of selection of passive components

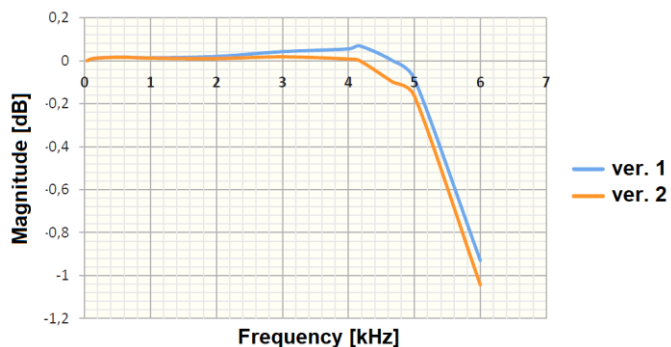


Fig. 8. Pass-band filter frequency response for TLV2462 and OP275 operational amplifiers in two versions of selection of passive components

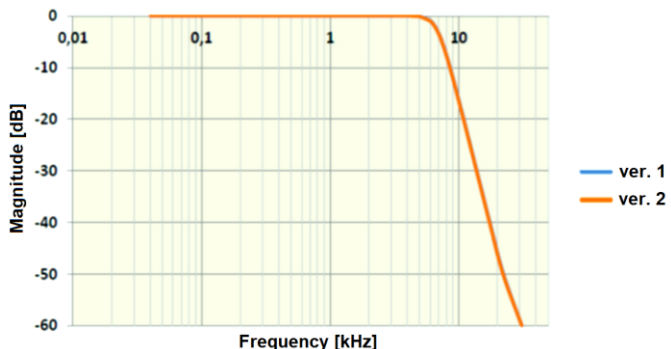


Fig. 9. Full-range filter frequency response for TLV2462 and OP275 operational amplifiers in two versions of selection of passive components (both curves are almost identical and overlap)

Version 1 of the reconstruction filter with TLV2462 operational amplifiers that realize the first part of the filter and the OP275 operational amplifiers that realize the second part of the filter was selected for the final implementation of the signal controller.

### B. Signal generation

The proposed generation method is stable and allows for very accurate setting of the signal frequency. Additionally, if the clock system clocking the DAC has a deviation of the sampling period  $T_s$  from the nominal value, it is possible to eliminate it by means of a constant (3) correction. In the presented generator,  $T_s$  is determined by the clock signal from the STM32F334R8 microcontroller, stabilized by a quartz resonator. After introducing the constant (3) correction, the maximum relative error of the signal frequency setting is less than  $10^{-5}$ , and therefore all the displayed frequency digits (c.f. Fig. 5 and Fig. 6) are accurate.

Figure 10 shows oscillograms of the stationary field and the signal that generate the counter-clockwise turning magnetic field.

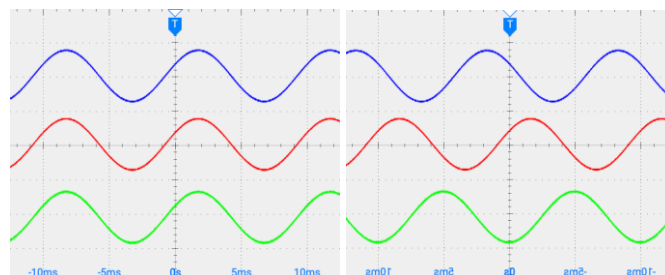


Fig. 10. Oscillograms of the 3-phase output signal for: a) stationary magnetic field, b) counter-clockwise turning magnetic field

Based on other physiotherapy devices, it was decided to ensure a slow increase and decrease of the signal power at the start and end of generation (so called soft-start and soft-stop function). This was implemented in the controller system, which linearly changes the settings of the signal amplitude and DC component during generation. If there is a DC component in the signal, then during soft-start the signal amplitude first increases gently and then the DC component is changed also gently. When the soft-stop function is working, the order of changes is reversed. Example oscillograms are presented in Fig. 11 and Fig. 12.

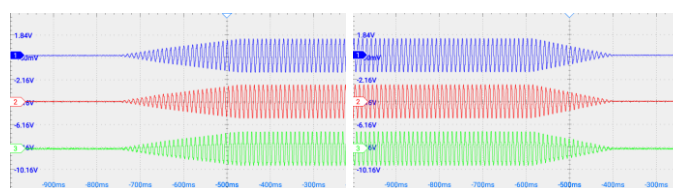


Fig. 11. 3-phase signals without DC component during soft start (left) and soft-stop (right)

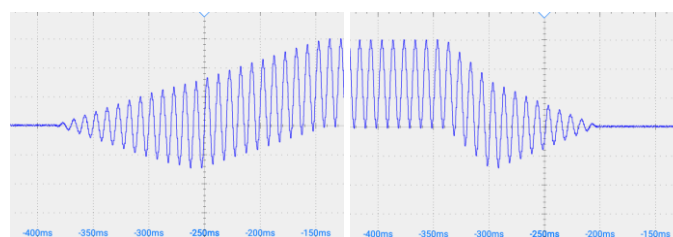


Fig. 11. Signal of one phase with a positive DC component added during soft start (left) and soft-stop (right)

### C. Magnetic field generation

To generate a magnetic field for therapeutic purposes, a power amplifier and an applicator containing coils is needed. The power amplifier was developed by the authors but is beyond the scope of this article.

Since the presented device is innovative, to the authors' knowledge, there are no 3-phase powered medical applicators on the market. However, it is also possible to use ready-made applicators in two solutions: using of 3 separate applicators or modifying of a multi-coil applicator (e.g. from Bardomed). In the second case, the coil connection must be changed, because the original applicator is powered by a single signal. For the tests, the authors made an applicator themselves, which contains coils in a star configuration (Fig. 12).

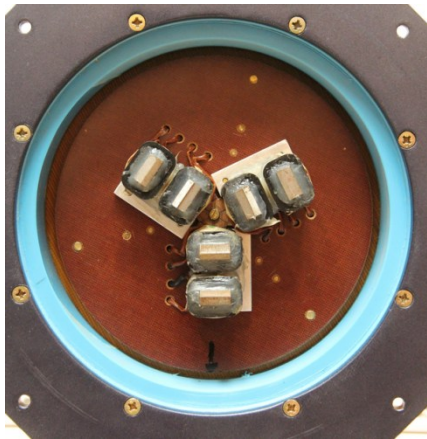


Fig. 12. View of the interior of a handmade magnetotherapy applicator (visible star configuration of coils)

## VII. CONCLUSIONS

The controller, taking into account the signal parameters and the stability and accuracy of the generation, works correctly, meeting the design assumptions.

The wide frequency range up to 5000 Hz imposed additional strong requirements on the applicators and the power amplifier, at the initial stage of the research it turned out to be unnecessary. For most applications, the range up to 1 kHz will probably be sufficient.

The controller operation is intuitive and the user interface is large and legible. During therapy, most often the therapist's attention is focused on the patient, so using a 5-inch touch screen without focusing attention on it can be difficult. For greater convenience of use, it is worth considering using a larger display or additional hardware buttons.

The proposed technique of simultaneous amplitude control and DC component addition, used in a signal path of the

controller, is universal and can be used in any bipolar signal generation system when a single-supply DAC is used.

The presented controller may be used for research and experimental work in the field of new techniques and applications of physical therapy.

## REFERENCES

- [1] T. Mika, W. Kasprzak, "Fizykoterapia," PZWL, Warszawa 2015
- [2] Astar, <https://astar.pl> (access: 30.03.2024).
- [3] A. Sieroń, G. Cielar, M. Adamek, "Magnetoterapia i laseroterapia niskoenergetyczna," Śląska Akademia Medyczna, Katowice 1993.
- [4] G. Straburzyński, A. Straburzyńska-Lupa, "Medycyna fizykalna," PZWL 1997.
- [5] BTL Polska Sp. z o.o., <https://www.btlnet.pl> (access: 30.03.2024).
- [6] I. Z. Samosiuk, W. Łyseniuk, A. Olszewska, "Praktyczne zastosowanie laseroterapii i laseropunktury w medycynie," OAiTL, Białystok 1996.
- [7] W. Glinkowski, L. Pokora, "Lasery w terapii," CTL, Warszawa 1993.
- [8] ZES Brno, a.s., "Výrobce magnetoterapeutických přístrojů Renaissance," <https://pulzni-magnetoterapie.cz> (access: 30.03.2024).
- [9] ZES Brno a.s., "RENAISSANCE Duo Forte – instruction manual," 2023.
- [10] P. Pawłowski, M. Portalski, H. Portalska, "Generacja wielotonów nieharmonicznych z wykorzystaniem procesorów sygnałowych (Generation of non-harmonic multitone signals by digital signal processors)," *Przegląd Elektrotechniczny (Electrical Review)*, R. 89, Nr 10/2013, pp. 122–125.
- [11] P. Pawłowski, R. Długosz, M. Radkowski, M. Wątyły, A. Dąbrowski, "Analog, Programmable Switched Capacitor FIR Filter Based on Rotator Architecture Implemented in CMOS," *SPA 2023 Signal Processing: Algorithms, Architectures, Arrangements, and Applications, Conference Proceedings, Poznan, 20th-22nd September 2023*, pp. 201–206, IEEE, 2023. <https://doi.org/10.23919/SPA59660.2023.10274431>
- [12] T. Marciniak, D. Cetnarowicz, P. Pawłowski, A. Dąbrowski, "Projektowanie filtrów analogowych do modułów cyfrowego przetwarzania sygnałów (Designing of analog filters for digital signal processing module)," *Przegląd Elektrotechniczny* 2019, R 95, nr 10, pp. 125–129, <https://doi.org/10.15199/48.2019.10.28>
- [13] M. Portalski, P. Pawłowski, A. Dąbrowski, "Synthesis of some class of nonharmonic tones," *XXVIII IC-SPETO Int. Conf. on Fundamentals of Electrotechnics and Circuit Theory*, vol. 2, pp. 439–442, 2005.
- [14] Arm, Mbed, "Rapid IoT device development," (access: 30.03.2024), <https://os.mbed.com/>
- [15] Texas Instruments, "TL07xx Low-Noise FET-Input Operational Amplifiers," SLOS080V, rev. April 2024, <https://www.ti.com/lit/ds/symlink/tl072.pdf>
- [16] D. Prasad, D. Tayal, A. Yadav, L. Singla, Z. Haseeb, "CNTFET Based OTRA and its Application as Inverse Low Pass Filter," *International Journal of Electronics and Telecommunications*, Vol. 65, pp. 665–670, No. 4 (2019), <https://doi.org/10.24425/ijet.2019.129826>
- [17] Texas Instruments, "TLV246x, Family of Low-Power Rail-to-Rail Input/Output Operational Amplifiers with Shutdown, SLOS220J, rev. Feb. 2004, <https://www.ti.com/lit/ds/symlink/tlv2462.pdf>
- [18] Analog Devices, "OP275 Dual Bipolar/JFET, Audio Operational Amplifier," rev. C, 2004, <https://www.analog.com/media/en/technical-documentation/data-sheets/OP275.pdf>